Proceedings of the International Symposium on Physics of Materials (ISPMA13)

Superplastic Behaviour of an Mg–Ag–RE Magnesium Alloy

Z. Trojanová[a,*], S. Chiappa[b], P. Málek[a], Z. Száraz[a,†], P. Lukáč[a] and T. Ryspaev[c]

[a]Faculty of Mathematics and Physics, Charles University in Prague, Ke Karlovu 3, 121 16 Praha 2, Czech Republic

[b]Department of Mechanical Engineering, Marche Polytechnic University, Via Brecce Bianche, 60131-Ancona, Italy

[c]Kyrgyz State Technical University, Kyrgyz-German Technical Institute, Bishkek, Kyrgystan

Fine-grained magnesium alloy QE22 (Mg–2.5wt.%Ag–2.5wt.%RE–0.6wt.%Zr) was prepared from cast ingot which was submitted to a two stages heat treatment. Subsequently the billet was overaged and extruded at high temperature. Samples were deformed at elevated temperatures from 380 °C up to 480 °C at various strain rates. Microstructure of deformed samples was studied using light and electron microscopy. Conditions for superplasticity of the investigated alloys have been estimated. Possible deformation mechanisms are discussed.

DOI: 10.12693/APhysPolA.128.765

PACS: 81.05.Bx, 62.20.fq

1. Introduction

Magnesium alloys containing rare earth (RE) elements are interesting for many industrial applications because of their low density and good mechanical properties, such as high specific strength at room and elevated temperatures, creep resistance and machinability. The addition of RE elements with Ag remarkably improves mechanical properties due to the existence of thermally stable precipitates [1]. Ageing causes precipitation within the grains. The decomposition of the supersaturated solid solution starts with the formation of coherent GP zones. It proceeds with the precipitation of two metastable hardening phases, and it gives rise to the formation of a stable precipitate at high temperature [2]. On the other hand, magnesium alloys with their hexagonal close packed structure exhibit lower ductility especially at lower temperatures. It is due to the limited number of slip systems for easy glide in the basal plane. To fulfil the von Mises criterion slip in a non-basal glide system is necessary [3]. The high critical resolved shear stress is the main reason for the limited ductility of magnesium alloys at lower temperatures. One way to overcome this restriction is to find conditions for superplastic deformation. In the superplastic region ductility of materials significantly increases and deformation process runs under a very small stress. Superplasticity of magnesium alloys of AZ series was reported in several papers for example [4–6]. On the other hand, superplasticity of magnesium alloys containing rare earth elements was studied only rarely [7–9]. In order to find conditions for superplastic forming without complicated fine-grained processing and increase application value, the superplastic behaviour and microstructure evolution of thermo-mechanically treated QE22 magnesium alloy have been investigated in the present paper.

*corresponding author; e-mail: ztrojan@met.mff.cuni.cz

†Present address: Institute for Energy, Joint Research Centre, European Commission, P.O. Box 2, 1755ZG Petten, The Netherlands.

2. Experimental

Commercial QE22 (2.5Ag–2.5RE–0.7Zr–balance Mg, in wt.%) was used in this study. As cast billets were heat-treated in two stages followed with hot extrusion. The thermo-mechanical processing consists of the subsequent steps: solution treatment at 470 °C for 10 h quenched in air; and overageing at 380 °C for 10 h followed warm extrusion at a temperature of 350 °C to obtain rods. Tensile specimens with a gauge length of 10 mm and a gauge diameter of 6 mm were machined with the tensile axis parallel to the extrusion direction. Abrupt strain-rate jump tests in tension and tensile tests with a constant crosshead speed were carried out using an Instron 5582 universal testing machine. The deformation tests were carried out at 420, 450, and 480 °C. Experiments at 420 °C were performed at constant strain rates in an interval from 7×10^{-5} to 1.3×10^{-2} s^{-1}. Tensile tests at 450 and 480 °C were realized with a constant machine speed. The strain rate sensitivity parameter m, defined as $m = \left(\frac{d \ln \sigma}{d \ln \dot{\varepsilon}}\right)_T$ was measured using the abrupt strain rate change test [10]. The furnace temperature was controlled with an accuracy of ±1 °C. The microstructure of the extruded and deformed alloys was observed by light microscope OLYMPUS and scanning electron microscope TESCAN VEGA LMU II. The resulting material after homogenization, precipitation ageing and hot extrusion exhibited a grain size of 6.1 μm.

The substructures of the specimens were examined using JEOL 2000FX transmission electron microscope operated at 200 kV. Foils for transmission electron microscopy (TEM) investigation were prepared by ion thinning with help of Technoorg Linda unit IV3/H system ion miller under small incidence angle of ion beam (to avoid artifacts in the substructure of the foils) and a voltage of 4–5 kV between cathodes.

3. Results and discussion

Microstructure of the as cast QE22 alloy consists of α-grains (solid solution of alloying elements in Mg) decorated at grain boundaries by the second phase particles (Fig. 1a). TEM revealed chains of smaller particles

containing Nd and Ag located mainly at grain boundaries (see Fig. 1b), only few particles were found inside of grains. These particles were dissolved during homogenisation annealing (470 °C for 10 h). TEM showed only groups of smaller and bigger non-dissolved zirconium particles. These Zr particles are very stable and they were not influenced by the homogenisation treatment. Small particles situated in grain boundaries were found after thermomechanical treatment (Fig. 1c). Very high stability of the grain structure is supported by the stable Mg3 (Ag, Nd) particles.

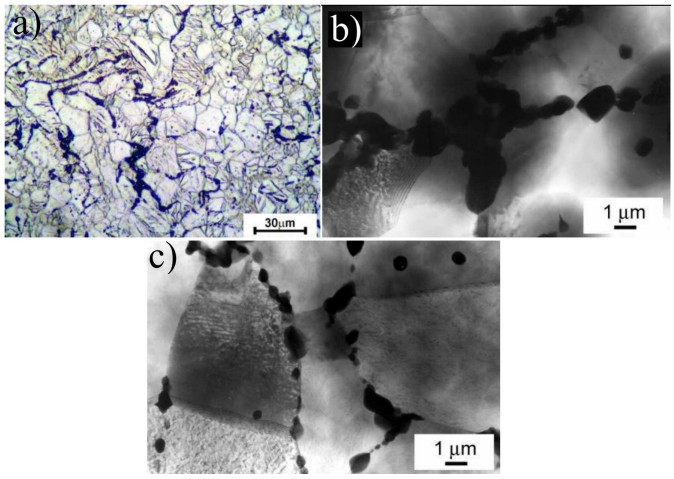

Fig. 1. Microstructure of the alloy: (a) light micrograph of the as prepared material consisting of α grains (light) and second phase particles (dark) situated mainly in grain boundaries, (b) TEM micrograph of the as cast alloy showing particles of Mg_3 (Ag, Nd) phase in grain boundaries, (c) TEM micrograph of the alloy after thermo-mechanical treatment showing particles of Mg_3 (Ag, Nd) phase located mainly in grain boundaries.

High values of the strain rate sensitivity of the flow stress, m, represent one of the main features of superplastic deformation. The high values of m as well as the elongation to failure, ε_f, are observed only in a certain region of the strain rates and temperatures. The values of the strain rate parameter, m, estimated for various strain rates and temperatures at three temperatures are introduced in Fig. 2a. A strong strain rate dependence of the m-parameter is obvious from Fig. 2a. Usually the m value of 0.3 is considered as a limit of the superplastic behaviour i.e. superplastic deformation should be limited to strain rates between 74×10^{-5} and 1×10^{-3} s^{-1} for temperatures $0.5-0.7T_M$ (where T_M being the melting point in [K]). Elongations to fracture obtained at various deformation temperatures for samples aged at three temperatures are introduced in the Table. Note that values estimated at 420 °C were obtained at a constant strain rate.

Microstructure analysis of samples deformed at 450 and 480 °C showed many cavities and deformation twins. The original grain size of ≈6 μm slightly increased during

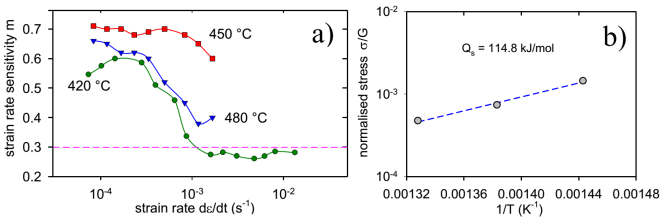

Fig. 2. Results of mechanical tests: (a) strain rate dependences of the strain rate sensitivity parameter m estimated for three temperatures, (b) plot of normalised stress σ/G vs. $1/T$.

TABLE

Maximum strain rate sensitivity, m(max), grain size after high temperature deformation, d_m, elongation to fracture, ε_f estimated for various temperatures.

T_D [°C]	m (max)	d_m [μm]	ε_f [%]	$\dot{\varepsilon}$ [s^{-1} × 10^{-4}]
420	0.60		490*	2.0
450	0.71	15.1	880	3.3
480	0.66	23.0	910	3.3

deformation to 15.1 μm at 450 °C and 23 μm at 480 °C but uniaxial shape of grains remained.

The surface of the sample deformed at 450 °C is introduced in Fig. 3b. Second phase particles and oxides which were formed during high temperature deformation are visible. Deformation twins and GBS are in the micrograph indicated by the light arrows. Bands visible at the surface are the traces of glide planes. These planes are very probably basal planes. Several authors observed (for example [11]) that during extrusion process a special texture is formed in hexagonal materials. The basal planes are oriented parallel to the extrusion direction (and also tension direction). Rotation of grains and free surface of the sample enabled formation of observed pattern.

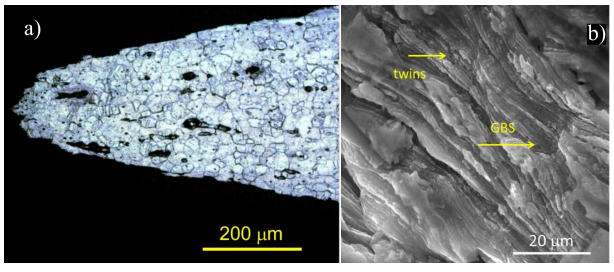

Fig. 3. Deformation features: (a) tip of the sample deformed at 480 °C (light micrograph), (b) surface wrinkles after deformation at 450 °C (SEM).

Strain rate $\dot{\varepsilon}$ of materials deformed at high temperatures is expressed by a relationship of the form

$$\dot{\varepsilon} = A\frac{Gb}{kT}\left(\frac{b}{d}\right)^p\left(\frac{\sigma}{G}\right)^n D, \qquad (1)$$

where A is a dimensionless material constant, G shear modulus, b is the Burgers vector of dislocations, d the grain size, p the grain size exponent, $n = 1/m$ is the

true stress exponent. kT has its usual meaning. D is the diffusion coefficient ($= D\exp(-Q/RT)$, where D the frequency factor, Q the activation energy for the diffusion process and R the gas constant), Steady state plastic flow of coarse-grained metals at high temperatures, above $0.4T_M$, is usually described by dislocation motion and storage on obstacles. These obstacles may be either of non-dislocation type as well as of dislocation type. As the obstacles of the non-dislocation type grain boundaries, incoherent precipitates or twin boundaries are considered. Steady state character of deformation is the consequence of equilibrium between hardening and recovery processes. Dislocation cross slip and climbing of dislocation may be considered as softening processes. In the fine grained materials two other independent mechanisms — grain boundary sliding accommodated by slip and directional diffusional flow may be considered [12, 13]. Each of the three deformation mechanisms has specific values of n, p, and Q by which the mechanism can be uniquely defined. For the plastic flow by slip of dislocation the high values of the stress exponent ($n = 5$ or higher) are characteristic and the activation energy is close to values for the activation energy of the lattice diffusion or for the pipe diffusion. The grain size exponent p is close to zero [14]. Grain boundary sliding accommodated (GBS) by dislocation slip or diffusional flow is characterised by the low values of the stress exponent (lower than 3 and 1 in the case of ideal superplasticity) and the activation energy is equal to the lattice or grain boundary diffusion or combination of both. Maximum estimated value of the stress sensitivity parameter exhibits 1.43. In order to understand the deformation mechanisms during superplastic process, the apparent superplastic deformation activation energy Q_s may be calculated [15]:

$$Q_s = \frac{1}{m} R \frac{\Delta \ln\left(\frac{\sigma}{G}\right)}{\Delta\left(\frac{1}{T}\right)}. \tag{2}$$

The shear modulus is given by the relationship

$$G = 1.66 \times 10^4 \left[1 - 0.49\left(\frac{T - 300}{924}\right)\right]. \tag{3}$$

The normalised stress σ/G plotted vs. $1/T$ is introduced in Fig. 2b. The activation energy estimated using Eq. (2) exhibits 114.8 kJ/mol. The activation energy estimated for volume diffusion in Mg is 135 kJ/mol and for grain boundary diffusion 92 kJ/mol [16]. It has been shown by Arzt et al. [17] that the overcoming of intergranular precipitates by grain boundary dislocation leads to higher activation energy. The deformation mechanism is considered to be GBS accommodated by slip controlled by lattice and grain boundary diffusion. Twinning as an accommodating mechanism may not be excluded. Observed deformation twinning may be considered as an additional accommodation mechanism. Documented grain growth prevent the diffusional accommodation process/(es) and lead to the formation of cracks.

4. Conclusions

Fine grained Mg–Ag–RE alloy was prepared with a special thermo-mechanical treatment. The grain size refinement may be attributed to very stable Mg_3 (Ag, Nd) phase situated in grain boundaries formed during the preparation process. Tensile deformation was performed at three temperatures from 420 to 480 °C. The maximum elongation was estimated for the strain rates in the order 10^{-4} s^{-1}, where also the maximum of the strain sensitivity was found. Superplastic deformation is realized by grain boundary sliding accommodated by lattice/grain boundary diffusion and mechanical twinning.

Acknowledgments

Z.T. and P.L. are grateful for the financial support of the Czech Science Foundation (project P204/12/1360).

References

[1] L.L. Rokhlin, *Magnesium Alloys Containing Rare Earth Metals: Structure and Properties*, Taylor & Francis, London 2003.

[2] G. Barucca, R. Ferragut, D. Lussana, P. Mengucci, F. Moia, G. Riontino, *Acta Mater.* **57**, 4416 (2009).

[3] R. von Mises, *Z. Angew. Math. Mech.* **8**, 161 (1928).

[4] Z. Trojanová, K. Turba, Z. Száraz, T. Ryspaev, P. Palček, M. Chalupová, *Acta Phys. Pol. A* **122**, 597 (2012).

[5] J.C. Tan, M.J. Tan, *Mater. Sci. Eng. A* **339**, 81 (2003).

[6] Y.H. Wei, Q.D. Wang, Y.P. Zhu, H.T. Zhou, W.J. Ding, Y. Chino, M. Mabuchi, *Mater. Sci. Eng. A* **360**, 107 (2003).

[7] V. Wesling, T. Ryspaev, A. Schram, *Mater. Sci. Eng. A* **462**, 144 (2007).

[8] T. Ryspaev, Z. Trojanová, O. Padalka, V. Wesling, *Mater. Lett.* **62**, 4041 (2008).

[9] K. Nakashima, H. Iwasaki, K.T. Mori, M. Mabuchi, M. Nakamura, T. Asahita, *Mater. Sci. Eng. A* **293**, 15 (2000).

[10] F. Booeshaghi, H. Garmestani, *Scr. Mater.* **40**, 509 (1999).

[11] H. Somekawa, T. Mukai, *Scr. Mater.* **53**, 541 (2005).

[12] A.K. Mukherjee, *Mater. Sci. Eng.* **8**, 83 (1971).

[13] T.G. Langdon, *Mater. Sci. Eng. A* **174**, 225 (1994).

[14] A.K. Mukherjee, J.E. Bird, J.E. Dorn, *Trans. Am. Soc. Met.* **62**, 155 (1969).

[15] S.W. Lee, Y.L. Chen, H.Y. Wang, C.F. Yang, J.W. Yeh, *Mater. Sci. Eng. A* **464**, 76 (2007).

[16] H.J. Frost, M.F. Ashby, *Deformation-Mechanism Maps*, Pergamon Press, Oxford, UK 1982, p. 44.

[17] F. Arzt, M.F. Ashby, R.A. Verral, *Acta Metall.* **31**, 1977 (1983).